# A Study of Transmission Mechanism for 2.45 GHz Wireless Body Area Networks

\*Takayuki Sasamori <sup>1</sup>, Masaharu Takahashi <sup>2</sup>, and Toru Uno <sup>3</sup>

Department of Electronics and Information Systems, Akita Prefectural University Yurihonjo, 015-0055 Japan, sasa@akita-pu.ac.jp

Research Center for Frontier Medical Engineering, Chiba University Chiba, 263-8522 Japan, masa@ieee.org

Faculty of Engineering, Tokyo University of Agriculture and Technology Koganei. 184-8588 Japan, uno@cc.tuat.ac.ip

# 1. Introduction

As one of the development of the future wireless communication systems, body-centric wireless communication using a device including a radio terminal placed in/on body is proposed [1]-[3]. In order to realize the wearable devices for the body-centric communications, it is apparent that examination of the antennas and propagation in the vicinity of the human body is very important.

In this paper, in order to investigate the transmission mechanism of the wearable device for on-body wireless communications analytically, we derive the eigenfunction solution and high frequency asymptotic representation for the scattered electromagnetic fields by a dielectric cylinder and discuss them. By comparing the high frequency asymptotic solution to the eigenfunction solutions for the scattered field in detail, the composition of the scattered fields are treated.

# 2. Formulation of the Problem

# 2.1 Eigenfunction Solution

Hence the propagation characteristic by the wearable device attached to an arm is considered, we approximate the arm as an infinite length dielectric circular cylinder. The geometry of the problem for the dielectric circular cylinder of radius a in the free space is illustrated in Fig. 1. The permittivity, the permeability and the conductivity are  $\varepsilon$ ,  $\mu$ ,  $\sigma$  for the dielectric cylinder, respectively. The permittivity and the permeability of the free space are  $\varepsilon_0$ ,  $\mu_0$ , respectively. A dipole antenna which is in the vicinity of the dielectric cylinder is placed coincident with the r direction in the cylindrical coordinate system. The length of the dipole antenna is  $l_1$  and the maximum amplitude of the current on the antenna is  $I_1$ . The center of the dipole antenna is located at  $Q(r_1, \phi_1, z_1)$ , and the observation point is located at  $P(r, \phi, z)$  in the cylindrical coordinate system.

When the cylinder described above is illuminated by a radiation electromagnetic wave from the dipole antenna, the frequency domain scattered field observed  $P(r, \phi, z)$  can be represented by the eigenfunction solution [4],[5]. By separation of the variables in Maxwell's equations and by imposing the boundary conditions on the cylinder surface r = a, one obtains the series solutions for the  $\phi$  components of magnetic scattered field  $H_{\phi}^{s}$ , as follows

$$H_{\phi}^{s} = -\frac{jI_{1}}{8\pi} \int_{-\infty}^{\infty} dh \sum_{n=0}^{\infty} \frac{2-\delta_{0}}{\eta^{2}} e^{-jh(z-z_{1})} \cos n(\phi - \phi_{1})$$

$$\left[ P_{n}(\lambda) \left\{ -A_{n} \frac{jhn}{r} H_{n}^{(2)}(\eta r) + B_{n} k_{0} \dot{H}_{n}^{(2)}(\eta r) \right\} + Q_{n}(\lambda) \left\{ -C_{n} jh \dot{H}_{n}^{(2)}(\eta r) + B_{n} \frac{h^{2}n}{k_{0}r} H_{n}^{(2)}(\eta r) \right\} \right]$$
(1)

where  $P_n(\lambda)$  and  $Q_n(\lambda)$  are uniform currents on the dipole antenna,

$$P_n(\lambda) = \int_{r_1 - l_1/2}^{r_1 + l_1/2} \frac{1}{r'} H_n^{(2)}(\eta r') dr', \tag{2}$$

$$Q_n(\lambda) = \int_{r_1 - l_1/2}^{r_1 + l_1/2} \dot{H}_n^{(2)}(\eta r') dr', \tag{3}$$

 $k_0$  is the free space wavenumber,  $\delta_0$  denotes the kronecker delta function defined by

$$\delta_0 = \begin{cases} 1 & \text{when } n = 0 \\ 0 & \text{when } n \neq 0 \end{cases}$$
 (4)

 $\eta = \sqrt{k_0^2 - h^2}$ ,  $H_n^{(2)}(z)$  is the Hankel function of second kind, the dot on this function denotes partial differential  $\partial/\partial r$  and the other coefficients are shown in Appendix.

$$A_n = -\frac{J_n(u)}{H_n^{(2)}(u)} - \frac{2j}{\pi} \frac{T_n(u, w)}{\left\{ u H_n^{(2)}(u) \right\}^2 R_n(u, w)}$$
 (5)

$$B_n = -\frac{2j}{\pi} - \frac{1}{\left\{ u H_n^{(2)}(u) \right\}^2 R_n(u, w)} \frac{jhn}{k_0} \left( \frac{1}{u^2} - \frac{1}{w^2} \right)$$
 (6)

$$C_n = -\frac{J_n(u)}{H_n^{(2)}(u)} - \frac{2j}{\pi} \frac{S_n(u, w)}{\left\{ u H_n^{(2)}(u) \right\}^2 R_n(u, w)} \tag{7}$$

$$R_n(u,w) = S_n(u,w)T_n(u,w) - \left(\frac{hn}{k_0}\right)^2 \left(\frac{1}{u^2} - \frac{1}{w^2}\right)^2$$
 (8)

$$S_n(u,w) = \frac{H_n^{(2)'}(u)}{uH_n^{(2)}(u)} - \mu_1 \frac{J_n'(u)}{wJ_n(u)}$$
(9)

$$T_n(u,w) = \frac{H_n^{(2)'}(u)}{uH_n^{(2)}(u)} - \varepsilon_1 \frac{J_n'(u)}{wJ_n(u)}$$
(10)

where  $\varepsilon_1 = \varepsilon/\varepsilon_0$ ,  $\mu_1 = \mu/\mu_0$ ,  $u = \eta a = \sqrt{k_0^2 - h^2} a$ ,  $w = \sqrt{k_1^2 - h^2} a$ ,  $k_1 = k_0 \sqrt{\varepsilon_1 \mu_1}$ ,  $J_n(z)$  is the Bessel function, the prime on  $J_n$  and  $H_n^{(2)}$  denotes the derivative with respect to the argument.

#### 2.2 High Frequency Asymptotic Representations of the Solution

To find the far-zone field of scattered fields, we need only the asymptotic expression for the eigenfunction solutions. This expression can be found by the method of saddle-point integration. Assuming the  $\eta r$  is large compared to unity, the Hankel function can be approximated by its asymptotic expression; that is,

$$H_n^{(2)}(\eta r) \approx \sqrt{\frac{2}{\pi \eta r}} e^{-j\left(\eta r - \frac{2n+1}{4}\pi\right)}.$$
(11)

We now change the cylindrical variables into spherical variables by letting  $r = R\sin\theta$ ,  $z = R\cos\theta$ . Applying the method of saddle-point integration to the eigenfunction representations (1) which substituted (11), we obtain

$$H_{\phi}^{s} \approx -\frac{I_{1}}{4\pi} \sum_{n=0}^{\infty} (2 - \delta_{0}) j^{n} \cos n(\phi - \phi_{1}) \frac{e^{-jkR}}{R(k_{0} \sin \theta)}$$

$$\left\{ P_{n}(\lambda) \left( A_{n} \frac{jh_{0}n}{r} + B_{n} j\eta_{0}k_{0} \right) + Q_{n}(\lambda) \left( C_{n}h_{0}\eta_{0} - B_{n} \frac{h_{0}^{2}n}{k_{0}r} H_{n}^{(2)}(\eta r) \right) \right\}$$
(12)

where  $h_0 = k_0 \cos \theta$ ,  $\eta_0 = k_0 \sin \theta$ .

# 3. Numerical Results and Discussion

In Eqn. (1), it is roughly represented that the integral interval of  $|h_0| < k_0$  and  $|h_0| > k_0$  are contributions of a propagating wave and a quasi-static field, respectively. The high frequency asymptotic solution is included in the propagating wave, because the saddle point  $h_0 = k_0 \cos \theta$  is always in the integral interval of  $|h_0| \le k_0$ . The infinite length dielectric circular cylinder has the radius of a = 27.5 mm, the relative permittivity of  $\varepsilon_1 = 58.12$ , the relative permeability of  $\mu_1 = 1$  and the conductivity of  $\sigma = 1.69$ . These electric constant values are close to muscles at a frequency of 2.45 GHz [6]. The center of the circular cylinder is located at the origin. A dipole antenna with a length of 54 mm is placed coincident with the x axis and with its center at r = 57.5 mm. Extensive numerical computations have been performed for different observation points when the current on the dipole antenna is  $I_1 = 1$ .

In Figure 2, the high frequency asymptotic solution has been compared with the exact solution. The magnitude curves of the  $\phi$  component of the scattered magnetic field are calculated as a function of z, for two cases r=57.5 mm and r=200 mm. In the case of r=57.5 mm, the curves calculated from the asymptotic representations deviates slightly from the exact solution in the whole range of z (0 mm  $< z \le 250$  mm). The asymptotic solution for r=200 mm agrees with the exact solution quite well.

Figure 3 shows the contours of the constant value of the error rate of the high frequency asymptotic solution versus the observation point (r, z), when  $\phi = 0$ . The error rate is

Error rate = 
$$\frac{\text{High frequency asymptotic solution - Eigenfunction solution}}{\text{Eigenfunction solution}}$$
. (13)

It can be seen in this figure that the signal transmission channel could be mostly dealt with the contribution of the propagating wave. However, the dominant signal transmission channel includes not only the contribution of the propagating wave but also the contribution of the quasi-static field in the case where the observation point is in the vicinity of the cylinder.

#### 4. Conclusion

In this paper, the transmission mechanism of the wearable device for on-body wireless communications is argued by analytically. By reason of the propagation characteristic by the wearable device attached to an arm is considered, we have approximated the arm as a dielectric circular cylinder. It has been regarded that the signal transmission channel of a wearable device using the human body can be generally dealt with the contribution of the propagating wave. However, in the case where the observation point is in the vicinity of the body, the high frequency solution deviates from the eigenfunction solution, since the percentage of the contribution of the quasi-static field included in the scattered field is comparatively large. This result leads us to the conclusion that the dominant signal transmission channel includes not only the contribution of the propagating wave

#### References

- [1] T. G. Zimmerman, "Personal area networks: Near-field intra-body communication," IBM Systems Journal, vol. 35, no. 3&4, pp. 609-617, 1996.
- [2] J. Bernhard, P. Nagel, J. Hupp, W. Strauss, and T. von der Grün, "BAN--Body area network for wearable computing," Proc. 9th Wireless World Research Forum, July 2003. [Online]. Available: http://www.wireless-world-research.org/
- [3] P. Coronel, W. Schott, K. Schwieger, E. Zimmermann, T. Zasowski, H. Maass, I. Oppermann, M. Ran, and P. Chevillat, "Wireless body area and sensor networks," Proc. Wireless World Research Forum Briefings, Dec. 2004. [Online]. Available: http://www.wireless-world-research.org/
- [4] L. B. Felsen and N. Marcuvitz, *Radiation and Scattering of Waves*, Englewood Cliffs, USA, Prentice-Hall, 1973.

- [5] C. T. Tai, *Dyadic Green Functions in Electromagnetic Theory*, 2nd ed., New York, USA, IEEE Press, 1993.
- [6] S. Gabriel, R. W. Lau, C. Gabriel, "The dielectric properties of biological tissues: II. Measurements in the frequency range 10 Hz to 20 GHz," Phys. Med. Biol., vol.41, pp.2251-2269, 1996.

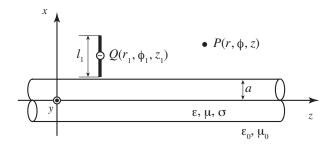


Figure 1 : Infinite dielectric circular cylinder, dipole antenna in free space and the coordinate system.

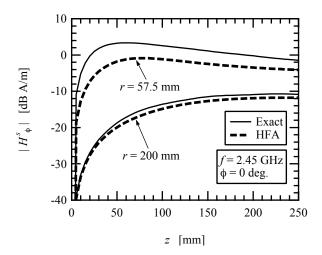


Figure 2 : Comparison of high frequency asymptotic solution and eigenfunction solution of  $H_{\phi}^{s}$  as a function of z.

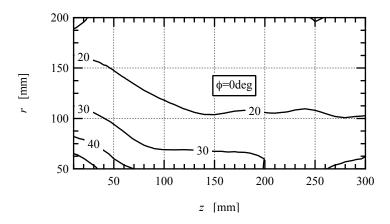


Figure 3 : Contours of error rate of high frequency asymptotic solution versus observation point (r, z), when  $\phi = 0$ .